Multibody Interaction Effects on Space Station Attitude Control and Momentum Management

Bong Wie*
Arizona State University, Tempe, Arizona 85287
and
Anren Hu† and Ramendra Singh‡
Dynacs Engineering Company, Inc., Clearwater, Florida 34623

The effects of multibody dynamic interaction on attitude control and momentum management of the Space Station Freedom are investigated, with emphasis on the impact of the mobile remote manipulator system and mobile transporter operations. In particular, the performance and stability of both classical and modern controllers are evaluated by nonlinear simulations of a rigid, two-body vehicle with the prescribed motion of the second body relative to the core body. It is shown that the mobile transporter maneuver with a large payload can significantly affect the overall system response, and in certain cases, the space station control system can become unstable. The instability, caused by more than 30% changes in the overall inertia property, indicates a need for an adaptive/robust control or gain scheduling for the large payload maneuvers.

Introduction

THE Space Station Freedom will employ control moment gyroscopes (CMG) as its primary actuating devices during normal flight mode operation. The use of a gravity-gradient torque is preferred for the CMG momentum management since it requires no consumables or additional hardware. For this reason, various control schemes using gravity-gradient torque were developed in Refs. 1-6. Furthermore, a full state feedback, multivariable, periodic-disturbance accommodating controller that is designed using the modern linear-quadratic-regulator (LQR) synthesis technique is currently being considered for actual implementation on the Space Station Freedom.[5,6]

In this paper, two of the proposed controllers (classical vs modern) are evaluated in detail to provide the control designer with options and approaches to meet the performance and stability requirements of the Space Station Freedom.[1] This paper provides an appropriate combination of mathematical modeling, classical and modern control synthesis, and discussion of multibody simulation results. The study objective is to validate the practicality of linear control synthesis approaches to multibody vehicles so that actual implementation of these linear controllers can be made with confidence on future multibody vehicles such as the Space Station Freedom.

Most current control system designs for the space station are based on a linearized equation of motion of a single, rigid body in a circular orbit. As illustrated in Fig. 1, however, the space station will be assembled and maintained using the mobile remote manipulator system (MRMS) and its mobile transporter (MT). The total weight of the MRMS/MT and its payload can be very large, possibly 30,000 lb or more. As the MRMS/MT carries a large payload, they will cause significant changes in the inertia property of the vehicle, which may affect the overall performance of the attitude control system in terms of pointing and stability. Hence, the multibody interaction effects on the control system design of the space station are of much current interest.[6,7]

In this paper, both classical and modern control designs are evaluated for such cases in which the MRMS/MT and its large payload travel along the surface of the vehicle, possibly 35 m (seven bays) away from the station's center of mass. There has not been a complete or detailed comparison of any proposed linear controllers in the presence of significant multibody dynamical interaction. This paper provides a detailed evaluation for such cases.

First, we review both the classical and modern control designs for a single rigid body in a circular orbit. Emphasis is given to different sets of equations for each design. We then discuss the equations of motion of a rigid, two-body system that can be considered a simplified model of the space station with the MRMS/MT maneuver. Finally, we present the simulation study results for the space station with the MRMS/MT operation. The impact of MRMS/MT operations is clearly identified with recommendations for a further detailed control system design.

Classical Multiloop Control Design

In this section, equations of motion of the space station in a circular orbit are discussed in terms of the total system momentum for the classical multiloop control design considered in Ref. 1. For simplicity, the space station is assumed to be a single, rigid body here. The rotating solar panels are not modeled, but the cyclic aerodynamic torque caused by the rotating solar panels is modeled as a prescribed external torque. Emphasis is placed on the use of the total system momentum expressed in the local vertical and local horizontal

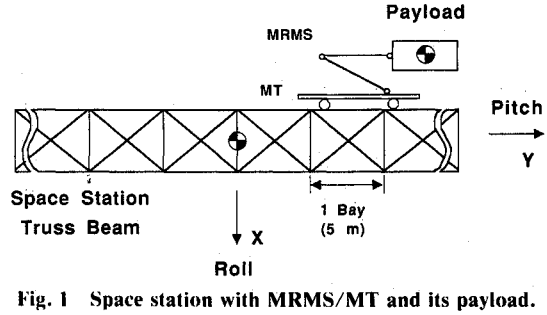

Fig. 1 Space station with MRMS/MT and its payload.

Received June 15, 1989; presented as Paper 89-3514 at the AIAA Guidance, Navigation, and Control Conference, Boston, MA, Aug. 14-16, 1989; revision received Dec. 12, 1989.

*Associate Professor, Department of Mechanical and Aerospace Engineering. Member AIAA.
†Research Scientist. Member AIAA.
‡President. Associate Fellow AIAA.

(LVLH) reference frame for feedback control. The x, y, z axes of the LVLH frame are the roll, pitch, and yaw axes, respectively, whose origin is fixed at the mass center, with the x axis in the flight direction, the y axis perpendicular to the orbit plane, and the z axis toward the Earth.

The equations of motion of the space station, expressed in the LVLH frame, can be written in matrix form as

$$\dot{\boldsymbol{H}} + \boldsymbol{\omega} \times \boldsymbol{H} = \boldsymbol{T}_{\text{ext}} \tag{1}$$

where $\boldsymbol{H} = [H_x\ H_y\ H_z]^T$ is the total system momentum of the space station, including the CMB momentum, expressed in the LVLH frame; $\dot{\boldsymbol{H}}$ is the rate of change of $\boldsymbol{H}$ as measured in the LVLH frame; $\boldsymbol{\omega} = [\omega_x\ \omega_y\ \omega_z]^T = [0, -n, 0]^T$ is the angular velocity of the LVLH frame that rotates with the orbital rate $n = 0.0011$ rad/s; T_{ext} is the sum of all the external torques, including gravity-gradient and aerodynamic torques, expressed in the LVLH frame; and the vector cross product $\times$ is defined as

$$\boldsymbol{\omega} \times \boldsymbol{H} \triangleq \begin{bmatrix} 0 & -\omega_z & \omega_y \\ \omega_z & 0 & -\omega_x \\ -\omega_y & \omega_x & 0 \end{bmatrix} \begin{bmatrix} H_x \\ H_y \\ H_z \end{bmatrix} \tag{2}$$

The gravity-gradient torque acting on the space station can be represented in the LVLH frame as

$$\boldsymbol{T}_{gg} \triangleq 3n^2 \boldsymbol{e} \times \boldsymbol{I}\boldsymbol{e} \tag{3}$$

where n is the orbital rate; $\boldsymbol{e} = [0, 0, -1]^T$ is the component of a unit vector directed from the Earth center to the mass center of the vehicle, expressed in the LVLH frame; $\boldsymbol{I}$ is the inertia matrix of the vehicle about the mass center, expressed in the LVLH frame.

Assume that the orientation of the vehicle's principal axes with respect to the LVLH frame is described by Euler angles of θ_x, θ_y, and θ_z. For small attitude deviations from the LVLH frame, the gravity-gradient torque can be approximated as

$$\boldsymbol{T}_{gg} = 3n^2 \begin{bmatrix} (I_3 - I_2)\theta_x \\ (I_3 - I_1)\theta_y \\ 0 \end{bmatrix} \tag{4}$$

where I_1, I_2, and I_3 are the principal moments of inertia of the vehicle about the body-fixed, principal-axis reference frame (1, 2, 3).

Combining Eqs. (1), (2), and (4), we get the equations of motion of the space station expressed in the LVLH frame

$$\begin{bmatrix} \dot{H}_x \\ \dot{H}_y \\ \dot{H}_z \end{bmatrix} = \begin{bmatrix} 0 & 0 & n \\ 0 & 0 & 0 \\ -n & 0 & 0 \end{bmatrix} \begin{bmatrix} H_x \\ H_y \\ H_z \end{bmatrix} + 3n^2 \begin{bmatrix} \Delta_x \theta_x \\ -\Delta_y \theta_y \\ 0 \end{bmatrix} + \begin{bmatrix} T_{ax} \\ T_{ay} \\ T_{az} \end{bmatrix} \tag{5}$$

where $\Delta_x = I_3 - I_2$, $\Delta_y = I_1 - I_3$; T_{ax}, T_{ay}, and T_{az} are the components of aerodynamic torque in the LVLH frame.

Note that the pitch equation about the y axis is decoupled from the roll/yaw equations about the x and z axes. As a result, control design can be performed separately for the pitch axis (out of plane) and the roll/yaw axes (in plane). The classical control design of Ref. 1 is based on a separation of inner attitude control and outer momentum control loops that are designed independently by using an analytical pole-placement technique. The control logic proposed in Ref. 1 for momentum management and attitude control can be summarized as follows.

Pitch Axis (out of Plane)

$$\dot{\theta}_{yc} = K_y(H_y - H_{yc}) - B_y\left[\theta_{yc} - K_b(H_{\text{CMG}y} + b\int H_{\text{CMG}y}\,dt)\right] \tag{6a}$$

$$\theta_{yc} = \int \dot{\theta}_{yc}\,dt \tag{6b}$$

$$T_{yc} = I_2\left[K_{Ry}(\dot{\theta}_y - \dot{\theta}_{yc}) + K_{Py}(\theta_y - \theta_{yc})\right] \tag{6c}$$

where θ_{yc} and $\dot{\theta}_{yc}$ are the pitch attitude and rate commands to the attitude controller [Eq. (6c)] from the momentum controller; T_{yc} is the pitch control torque command to the CMG; H_{yc} is the desired total system momentum command; $H_{\text{CMG}y}$ is the CMG momentum along the LVLH y axis; K_{Ry} and K_{Py} are the attitude controller gains; K_y, B_y, K_b, and b are the pitch-axis momentum controller gains. Note that the control torque command T_{yc} has an "adaptive" gain factor of I_2 for the time-varying pitch inertia.

Roll/Yaw Axis (in Plane)

$$\dot{\theta}_{xc} = K_x(H_x - H_{xc}) + K_z(H_z - H_{zc}) - B_x\left[\theta_{xc} - K_c(H_{\text{CMG}z} + c\int H_{\text{CMG}z}\,dt)\right] \tag{7a}$$

$$\theta_{xc} = \int \dot{\theta}_{xc}\,dt \tag{7b}$$

$$T_{xc} = I_1\left[K_{Rx}(\dot{\theta}_x - \dot{\theta}_{xc}) + K_{Px}(\theta_x - \theta_{xc})\right] \tag{7c}$$

$$\dot{\theta}_{zc} = K_d H_{\text{CMG}x} \tag{7d}$$

$$\theta_{zc} = \int \dot{\theta}_{zc}\,dt \tag{7e}$$

$$T_{zc} = I_3\left[K_{Rz}(\dot{\theta}_z - \dot{\theta}_{zc}) + K_{Pz}(\theta_z - \theta_{zc})\right] \tag{7f}$$

where $\dot{\theta}_{xc}$ and θ_{xc} are the roll rate and attitude commands, respectively; $\dot{\theta}_{zc}$ and θ_{zc} are the yaw rate and attitude commands, respectively; T_{xc} and T_{zc} are the roll and yaw control torque commands to the CMG, respectively; H_{xc} is the desired total system momentum command along the LVLH x and z axis; $H_{\text{CMG}x}$ and $H_{\text{CMG}z}$ are the CMG momentum along the LVLH x and z axes, respectively; K_{Rx}, K_{Px}, K_{Rz}, and K_{Pz} are the roll/yaw attitude controller gains; K_x, K_z, B_x, K_c, K_d, and c are the roll/yaw momentum controller gains.

The total system momentum of the space station $\boldsymbol{H}$ can be written in the LVLH frame as the sum of the angular momentum of the vehicle $\boldsymbol{H}_V$ and the CMG momentum $\boldsymbol{H}_{\text{CMG}}$; that is,

$$\boldsymbol{H} = \boldsymbol{H}_V + \boldsymbol{H}_{\text{CMG}} = \begin{bmatrix} I_1\dot{\theta}_x + n(I_2 - I_3)\theta_z \\ I_2(\dot{\theta}_y - n) \\ I_3\dot{\theta}_z + n(I_3 - I_2)\theta_x \end{bmatrix} + \begin{bmatrix} H_{\text{CMG}x} \\ H_{\text{CMG}y} \\ H_{\text{CMG}z} \end{bmatrix} \tag{8}$$

where $H_{\text{CMG}x}$, $H_{\text{CMG}y}$, and $H_{\text{CMG}z}$ are the CMG momentum components in the LVLH frame. Small Euler angles are assumed here.

The CMG momentum dynamics can also be described by

$$\dot{H}_{\text{CMG}x} - nH_{\text{CMG}z} = T_x \tag{9a}$$

$$\dot{H}_{\text{CMG}y} = T_y \tag{9b}$$

$$\dot{H}_{CMGz} + nH_{CMGx} = T_z \tag{9c}$$

where T_x, T_y, and T_z are the control torques generated by the CMG.

The classical control design for the space station momentum management, proposed in Ref. 1, is essentially based on a frequency separation between "slow" momentum control and "fast" attitude control. As a result, it can be assumed that $\theta_x \cong \theta_{xc}$, $\theta_y \cong \theta_{yc}$, and $\theta_z \cong {}_{zc}$. We also assume a perfect CMG steering law, i.e. $T_x \cong T_{xc}$, $T_y \cong T_{yc}$, and $T_z \cong T_{zc}$.

If we use Eqs. (6–9) and the aforementioned simplifying assumptions, the closed-loop characteristic equations of the momentum controllers can be written in terms of those gains in Eqs. (6) and (7). By selecting the desired closed-loop poles, the associated gains can be determined. The most unique feature of the control design in Ref. 1 is the use of an analytical pole-placement technique that accounts for the changing inertia property. The momentum controller gains can be calculated from the following equations, which can be simply implemented for the onboard computation of adaptive gains

$$B_x = 2\zeta_x\omega_x + 0.1 \tag{10a}$$

$$B_y = 2\zeta_y\omega_y \tag{10b}$$

$$K_x = \frac{n^2 - 0.2\zeta_x\omega_x - \omega_x^2}{3n^2\Delta_x} \tag{10c}$$

$$K_y = \frac{n^2}{3n^2\Delta_y} \tag{10d}$$

$$K_b = \frac{an^2}{3n^2b\Delta_y - an^2I_2B_y} \tag{10e}$$

$$K_c = \frac{(0.1a - a^2)(a^2 - 2\zeta_x\omega_x a + \omega_x^2)}{nB_x\Delta_x(a^2 + 4n^2)(c - a)} \tag{10f}$$

$$K_d = \frac{a}{n\Delta_z} \tag{10g}$$

where $\Delta_x = I_3 - I_2$, $\Delta_y = I_1 - I_3$, and $\Delta_z = I_2 - I_1$; ω_y and ζ_y are the natural frequency and damping ratio of the pitch momentum control loop, respectively; ω_x and ζ_x are the natural frequency and damping ratio of the roll/yaw momentum control loop, respectively. A controller to be called the "Honeywell" controller later in this paper has the following values for ω, ζ, a, b, and c: $\omega_y = 0.0006$ rad/s, $\zeta_y = 0.5$, $\omega_x = 0.002$ rad/s, $\zeta_x = 0.5$, $a = n/4\pi$, $b = 0.001$, and $c = 0.0003$; and attitude controller gains of $K_{Rx} = K_{Ry} = K_{Rz} = 0.056$ and $K_{Px} = K_{Py} = K_{Pz} = 0.0016$ that correspond to the natural frequency of 0.04 rad/s and damping ratio of 0.7 for each axis.

Linear-Quadratic-Regulator Design

In this section, the equations of motion of the space station in a circular orbit are expressed in the body-fixed axes for the purpose of a full-state feedback, multivariable, periodic-disturbance accommodating control design using the linear-quadratic-regulator (LQR) synthesis technique. A LQR-based controller designed using a state-space model of the space station with a cyclic aerodynamic disturbance torque, developed in Refs. 3 and 4, is currently being considered for actual implementation on the Space Station Freedom.[5,6]

For such modern control designs, the linearized equations of motion of a single rigid body in a circular orbit can be described as follows.

Space Station Dynamics

$$\begin{bmatrix} I_{11} & I_{12} & I_{13} \\ I_{12} & I_{22} & I_{23} \\ I_{13} & I_{23} & I_{33} \end{bmatrix} \begin{bmatrix} \dot{\omega}_1 \\ \dot{\omega}_2 \\ \dot{\omega}_3 \end{bmatrix} =$$

$$+ n \begin{bmatrix} I_{13} & 2I_{23} & I_{33} - I_{22} \\ -I_{23} & 0 & I_{12} \\ I_{22} - I_{11} & -2I_{12} & -I_{13} \end{bmatrix} \begin{bmatrix} \omega_1 \\ \omega_2 \\ \omega_3 \end{bmatrix}$$

$$+ 3n_2 \begin{bmatrix} I_{33} - I_{22} & I_{12} & 0 \\ I_{12} & I_{33} - I_{11} & 0 \\ -I_{13} & -I_{23} & 0 \end{bmatrix} \begin{bmatrix} \theta_1 \\ \theta_2 \\ \theta_3 \end{bmatrix}$$

$$+ n^2 \begin{bmatrix} -2I_{23} \\ 3I_{13} \\ -I_{12} \end{bmatrix} + \begin{bmatrix} -u_1 + w_1 \\ -u_2 + w_2 \\ -u_3 + w_3 \end{bmatrix} \tag{11}$$

Attitude Kinematics

$$\dot{\theta}_1 - n\theta_3 = \omega_1 \tag{12a}$$

$$\dot{\theta}_2 - n = \omega_2 \tag{12b}$$

$$\dot{\theta}_3 + n\theta_1 = \omega_3 \tag{12c}$$

CMG Momentum Dynamics

$$\dot{h}_1 - nh_3 = u_1 \tag{13a}$$

$$\dot{h}_2 = u_2 \tag{13b}$$

$$\dot{h}_3 + nh_1 = u_3 \tag{13c}$$

where ω_1, ω_2, and ω_3 are the body-axis components of the absolute angular velocity of the space station, called the roll, pitch, and yaw body rates, respectively; I_{ij} $(i = j)$ are the moments of inertia; I_{ij} $(i \neq j)$ are the products of inertia; h_1, h_2, and h_3 are the body-axis components of the CMG momentum; u_1, u_2, and u_3 are the body-axis components of the control torque; w_1, w_2, and w_3 are the body-axis components of the external disturbance torque; and n is the orbital rate of 0.0011 rad/s.

Most practical situations with small products of inertia permit the further simplification of Eq. (11), resulting in the following equations:

$$\begin{aligned} I_1\dot{\omega}_1 + n(I_2 - I_3)\omega_3 + 3n^2(I_2 - I_3)\theta_1 &= -u_1 + w_1 \\ I_2\dot{\omega}_2 + 3n^2(I_1 - I_3)\theta_2 &= -u_2 + w_2 \\ I_3\dot{\omega}_3 - n(I_2 - I_1)\omega_3 &= -u_3 + w_3 \end{aligned} \tag{14}$$

where $I_i \triangleq I_{ii}$ for $i = 1, 2, 3$.

Combining Eqs. (12) and (14), we get

$$I_1\ddot{\theta}_1 + 4n^2(I_2 - I_3)\theta_1 - n(I_1 - I_2 + I_3)\dot{\theta}_3 = -u_1 + w_1 \tag{15a}$$

$$I_2\ddot{\theta}_2 + 3n^2(I_1 - I_3)\theta_2 = -u_2 + w_2 \tag{15b}$$

$$I_3\ddot{\theta}_3 + n^2(I_2 - I_1)\theta_3 + n(I_1 - I_2 + I_3)\dot{\theta}_1 = -u_3 + w_3 \tag{15c}$$

These are the well-known equations used for the study of the passive and/or active gravity-gradient stabilization of Earth-pointing satellites (e.g., see Ref. 11). Since pitch motion is uncoupled from roll/yaw motion, pitch control is often treated separately from the coupled roll/yaw control. The aerodynamic disturbances are modeled as a bias plus periodic

Table 1 Inertia property[a]

	Space station	Payload
Weight, lb	300,000	30,000
I_{11}	50.28E6	1.94E5
I_{22}	10.80E6	2.60E5
I_{33}	58.57E6	1.94E5
I_{12}	−3.90E5	0.0
I_{13}	−2.40E5	0.0
I_{23}	1.60E5	0.0

[a]Inertia in units of slug-ft^2.

terms in the body-fixed axes

$$w(t) = \text{Bias} + A_n \sin(nt + \phi_1) + A_{2n} \sin(2nt + \phi_2) + A_{3n} \sin(3nt + \phi_3) + A_{4n} \sin(4nt + \phi_4)$$

The dominant aerodynamic torque frequencies in n and $2n$ are caused by the Earth's diurnal bulge and solar panel rotation effects, respectively. Actual magnitudes and phases of these disturbance torques are assumed unknown for control design.

Pitch Control

A state-space control design for the pitch axis is described here. In Refs. 3 and 4 a periodic disturbance accommodating controller was developed to asymptotically control either pitch attitude or CMG momentum oscillations occurring at the frequencies present in the aerodynamic disturbance torques. The disturbance rejection filters for pitch attitude control can be represented as

$$\ddot{\alpha}_2 + (n)^2\alpha_2 = \theta_2$$
$$\ddot{\beta}_2 + (2n)^2\beta_2 = \theta_2$$
$$\ddot{\gamma}_2 + (3n)^2\gamma_2 = \theta_2$$
$$\ddot{\eta}_2 + (4n)^2\eta_2 = \theta_2$$

The pitch-axis control logic is then given by a single control input involving 12 states

$$u_2 = \boldsymbol{K}_{22}\boldsymbol{x}_2 \tag{16}$$

where $\boldsymbol{K}_{22}$ is a 1×12 gain matrix, and $x_2 \triangleq [\theta_2\ \dot{\theta}_2\ h_2 \int h_2\ \alpha_2\ \dot{\alpha}_2\ \beta_2\ \dot{\beta}_2\ \gamma_2\ \dot{\gamma}_2\ \eta_2\ \dot{\eta}_2]^T$. The control design task is to find proper gains for this 12-state feedback controller. If the cyclic aerodynamic torques at $3n$ and $4n$ components are not significant, the $3n$ and $4n$ filters may not be needed. As discussed in Ref. 4, however, these higher harmonic components in the pitch axis have some cross-coupling effects on roll/yaw momentum management.

For the pitch control design, various design techniques can be used, including the linear-quadratic-regulator (LQR) synthesis and pole-placement techniques. Several iterations of any method may be required to achieve satisfactory closed-loop performance and robustness. The open-loop pitch axis of the phase 1 space station with the inertia data given in Table 1 is unstable, with poles at $s = \pm 1.5n$, 0, 0, and filter poles at $s = \pm jn$, $\pm j2n$, $\pm j3n$, $\pm j4n$. One pole at $s = 0$ comes from the integral feedback of h_2. A typical LQR design and simulation results for this nominal case without MRMS/MT operation can be found in Refs. 3 and 4. As discussed in those papers, the pitch-axis controller of the phase 1 space station can become unstable with as little as a -7% variation in I_3 and $+8\%$ variation in I_1. It is, however, important to note that such small robustness with respect to inertia uncertainty is not related to the selection of LQR gains, but is the physical limitation inherent in gravity-gradient stabilization.

Roll/Yaw Control

The roll/yaw controller has a structure similar to that of the pitch controller. In Refs. 3 and 4, an inherent physical property of the coupled roll/yaw dynamics is investigated in terms of the transmission zeros of a multivariable system. As a result, a periodic disturbance at the orbital rate can be rejected in the yaw attitude but not in the roll attitude. Periodic-disturbance rejection filters for the asymptotic control of roll CMG momentum and yaw attitude can be represented as

$$\ddot{\alpha}_1 + (n)^2\alpha_1 = h_1$$
$$\ddot{\beta}_1 + (2n)^2\beta_1 = h_1$$
$$\ddot{\gamma}_1 + (3n)^2\gamma_1 = h_1$$
$$\ddot{\eta}_1 + (4n)^2\eta_1 = h_1$$
$$\ddot{\alpha}_3 + (n)^2\alpha_3 = \theta_3$$
$$\ddot{\beta}_3 + (2n)^2\beta_3 = \theta_3$$
$$\ddot{\gamma}_3 + (3n)^2\gamma_3 = \theta_3$$
$$\ddot{\eta}_3 + (4n)^2\eta_3 = \theta_3$$

The roll/yaw control logic involving two control inputs and 24 states is expressed as

$$\begin{bmatrix} u_1 \\ u_3 \end{bmatrix} = \begin{bmatrix} \boldsymbol{K}_{11} & \boldsymbol{K}_{13} \\ \boldsymbol{K}_{31} & \boldsymbol{K}_{33} \end{bmatrix} \begin{bmatrix} \boldsymbol{x}_1 \\ \boldsymbol{x}_3 \end{bmatrix} \tag{17}$$

where $\boldsymbol{K}_{ij}$ is a 1×12 gain matrix, $x_1 \triangleq [\theta_1\ \omega_1\ h_1 \int h_1\ \alpha_1\ \dot{\alpha}_1\ \beta_1\ \dot{\beta}_1\ \gamma_1\ \dot{\gamma}_1\ \eta_1\ \dot{\eta}_1]^T$, and $x_3 \triangleq [\theta_3\ \omega_3\ h_3 \int h_3\ \alpha_3\ \dot{\alpha}_3\ \beta_3\ \dot{\beta}_3\ \gamma_3\ \dot{\gamma}_3\ \eta_3\ \dot{\eta}_3]^T$.

The phase 1 space station roll/yaw axis is open-loop unstable, with poles at $s = \pm 1.05n$, $\pm j0.7n$, 0, 0, $\pm jn$, and filter poles at $s = \pm jn$, $\pm jn$, $\pm j2n$, $\pm j2n$, $\pm j3n$, $\pm j3n$, $\pm j4n$, $\pm j4n$. The double pole at $s = 0$ occurs because of the integral feedback of h_1 and h_3. A typical LQR design for this case can be found in Refs. 3 and 4, and its performance and stability during the MRMS/MT operation are investigated in this paper. The study results show that a partial-state feedback controller with $\boldsymbol{K}_{13} = \boldsymbol{K}_{31} = 0$, which was developed in Ref. 3 as an optional capability to reduce gain storage requirements, is more sensitive to inertia variations than the standard full-state, LQR-type controller. In Ref. 8, a LQR-based, pole-placement technique is also applied to the Space Station Freedom.

Equations of Motion for a Two-Body System

In this section, we derive the equations of motion for a rigid, two-body system consisting of the space station as the first body and the MRMS/MT with payload as the second body. For simplicity, we consider here only a prescribed translational/rotational motion of the second body relative to the first body.

As illustrated in Fig. 2, the total system C consists of a main body A with mass m_A and inertia matrix $\boldsymbol{I}_A$ about its mass

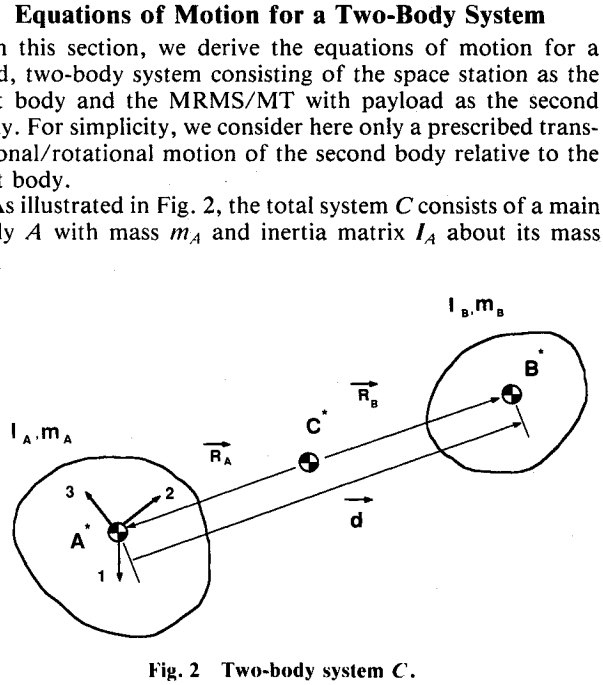

Fig. 2 Two-body system C.

center A^*, and a body B with m_B and inertia matrix I_B about its mass center B^*. The composite mass center is denoted by C^*, which is assumed to move in a circular orbit. The total system momentum about the composite mass center can be expressed in the reference frame fixed in the main body A

$$H = (I_A + I_B - m_A\tilde{R}_A^2 - m_B\dot{R}_B)\omega + m_A R_A \times \dot{R}_A + m_B R_B \times \dot{R}_B + H_{CMG} \tag{18}$$

where R_A represents the components of the position vector from C^* to A^*, expressed in the body A frame; R_B represents the components of the position vector from C^* to B^*, expressed in the body A frame; for each body, $R = [R_1\ R_2\ R_3]^T$; and

$$\tilde{R}^2 \triangleq \begin{bmatrix} 0 & -R_3 & R_2 \\ R_3 & 0 & -R_1 \\ -R_2 & R_1 & 0 \end{bmatrix}^2 \tag{19}$$

Since

$$R_A = \frac{-m_B}{m_A + m_B} d \tag{20a}$$

$$R_B = \frac{m_A}{m_A + m_B} d \tag{20b}$$

where d is the prescribed vector position from A^* to B^* expressed in the body A frame, we have the following relations:

$$m_A\ddot{R}_A^2 + m_B\ddot{R}_B^2 = \frac{m_A m_B}{m_A + m_B}\tilde{d}^2$$

$$m_A R_A \times \dot{R}_A + m_B R_B \times \dot{R}_B = \frac{m_A m_B}{m_A + m_B} d \times \dot{d}$$

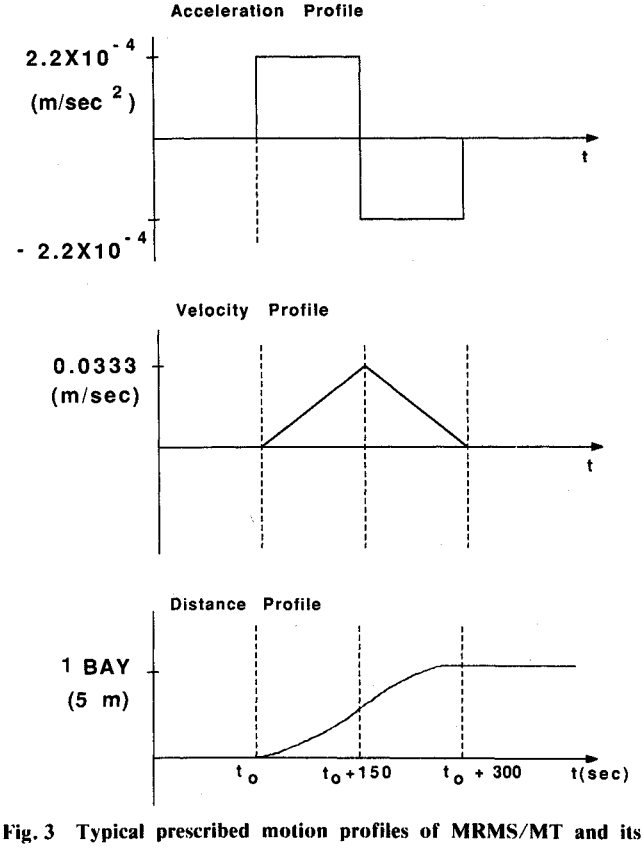

Fig. 3 Typical prescribed motion profiles of MRMS/MT and its payload.

where $d = [d_1\ d_2\ d_3]^T$; and

$$\tilde{d}^2 \triangleq \begin{bmatrix} 0 & -d_3 & d_2 \\ d_3 & 0 & -d_1 \\ -d_2 & d_1 & 0 \end{bmatrix}^2 \tag{21}$$

Thus, the total system momentum about the composite center of mass can be rewritten as

$$H = \left[I_A + I_B - \frac{m_A m_B}{m_A + m_B}\tilde{d}^2\right]\omega + \frac{m_A m_B}{m_A + m_B} d \times \dot{d} + H_{CMG} \tag{22}$$

where $m_A m_B/(m_A + m_B)$ is often called the reduced mass of the system. It can be seen that the prescribed relative motion $d(t)$ directly affects the total system momentum. Since the rate of change of angular momentum of a system is equal to the external torque acting on the system, the equations of motion can then be written as

$$\dot{H} + \omega \times H = T_{ext} \tag{23}$$

where $H = [H_1\ H_2\ H_3]^T$ is the total system momentum expressed in the body A frame; $\dot{H}$ is the rate of change of H as measured in the body A frame; $\omega = [\omega_1\ \omega_2\ \omega_3]^T$ is the angular velocity of the body A expressed in the body A frame; T_{ext} is the sum of all the external torques, including gravity-gradient and aerodynamic torques, expressed in the body A frame.

A typical prescribed motion profile of the MRMS/MT and its payload along the y axis of the station, shown in Fig. 3 for one bay maneuver, is discussed here. Each prescribed translation is divided into "bay maneuvers," where one bay consists of a 5-m truss beam. Suppose a four-bay maneuver along the y axis is prescribed. The entire maneuver may be considered as four individual maneuvers, each separated by a finite amount of time. Each individual maneuver is identical in the sense that the acceleration profile, and hence the velocity and displacement profile, are prescribed in the same way. It is assumed that one bay manuever takes 300 s to move 5 m.

Payload slewing is also modeled much the same way as the translation. The acceleration, velocity, and displacement profiles have similar but different slopes compared to the profiles for translation. A 180-deg slew maneuver is modeled as eight individual maneuvers, each slewing about 22.5 deg. The accelerations and rates used for the slew maneuver study in this paper are based on the accelerations and rates of the Space Shuttle's remote manipulator system (RMS) motion, with a maximum angular velocity of approximately one-half that of a loaded RMS joint.

The multibody computer code used in this study is a time-history simulation program for a rigid, multibody space station with active control elements. The function of this simulation code is to provide a rigorous environment for the design and analysis of a space station control system. The simulation program provides detailed environmental models for the orbiting space station, including aerodynamic drag, solar radiation pressure, gravity-gradient torque, Earth's magnetic field, and orbiting reference frames.

The space station is modeled as interconnected multibodies. The interface of each body consists of zero to three rotational degree-of-freedom joints that provide the definition of kinematic variables. In addition to the rotational degree-of-freedom joints, the program provides for the user-defined, prescribed relative motion (both translational and rotational) of a multibody system for simulating MRMS/MT operation. A detailed discussion of this multibody computer code and its computationally efficient algorithm can be found in Ref. 10.

In the next section, some simulation results for the space station with MRMS/MT operation are discussed.

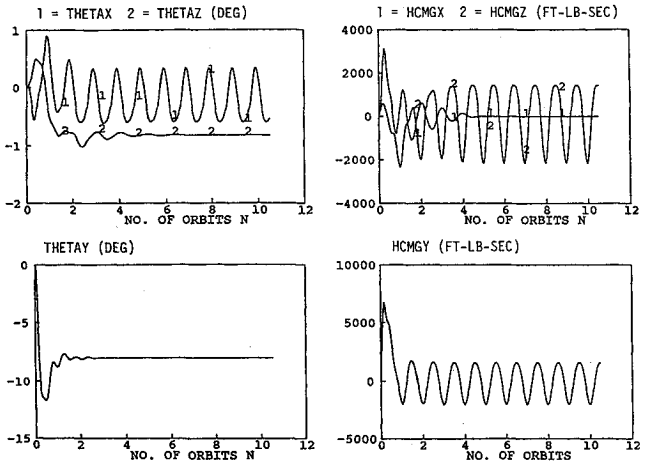

Fig. 4 Case I with the JSC controller.

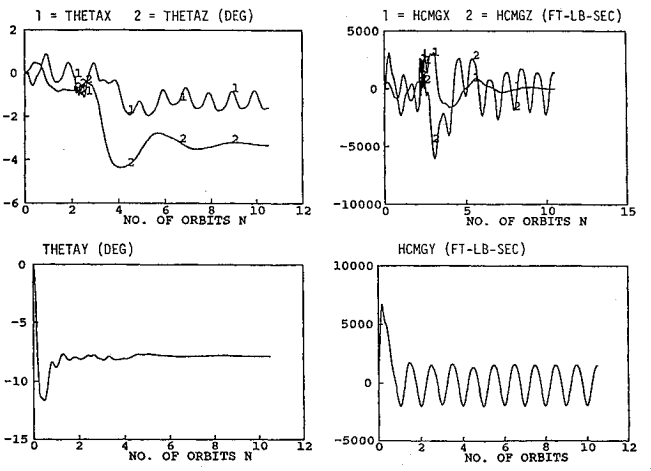

Fig. 6 Case II with the JSC controller.

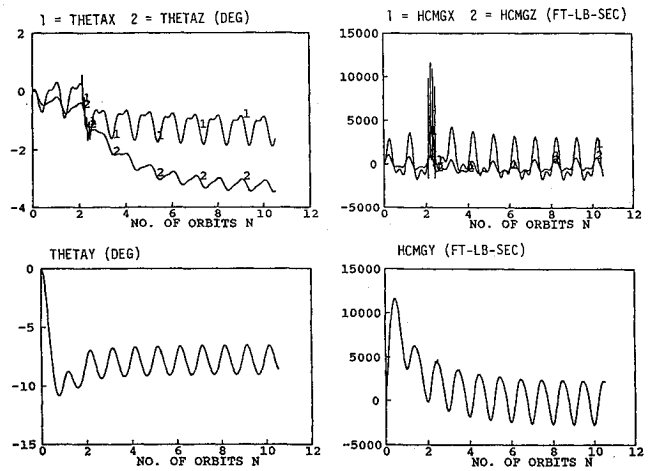

Fig. 5 Case II with the Honeywell controller.

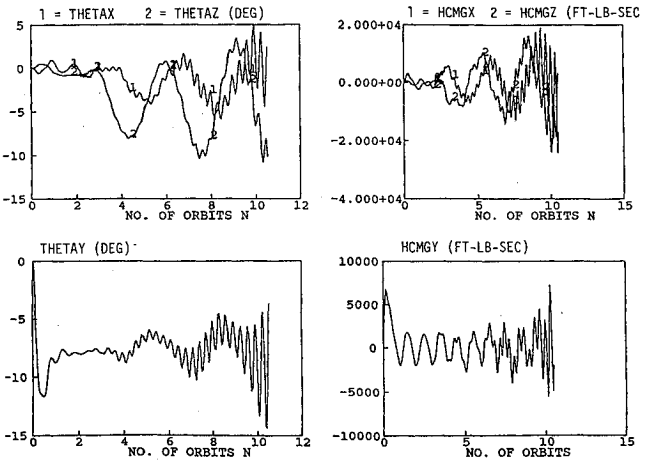

Fig. 7 Case III with the JSC controller.

Discussion of Simulation Results

This section gives a brief description of the different test cases used to evaluate the linear control algorithms of Refs. 1, 3, and 4, which were summarized in the previous sections of this paper. A detailed discussion of the simulation study results can be found in Ref. 9. Table 1 summarizes the mass properties of the space station and the MRMS/MT with a 30,000 lb payload. In the subsequent discussions, a controller discussed in Ref. 1 is called the "Honeywell" controller, whereas a control developed in Refs. 3 and 4 is called the "JSC (Johnson Space Center)" controller.

Case I: Nominal Case

Case I provides the baseline performance of the controllers with no MRMS/MT maneuver and a test case to verify controller algorithm implementation in a multibody simulation code. In this case, there are no significant differences between the Honeywell and JSC controllers except for the disturbance rejection capability of the JSC controller. In general, the responses of both controllers are acceptable, except for the steady-state attitude oscillations of the Honeywell controller, which are caused by cyclic aerodynamic torques. In Fig. 4, typical time responses of the JSC controller are shown for this case without the MRMS/MT maneuver. Pitch TEA (torque equilibrium attitude) is about -8 deg, yaw TEA is -0.8 deg, and roll dynamic TEA is -0.12 deg. Detailed discussions of the modern state-space LQR design for this nominal case can be found in Refs. 3 and 4.

Case II: Four-Bay Translation Along the Pitch Axis

Case II consists of a four-bay maneuver. (One bay maneuver takes 300 s to move 5 m.) The prescribed MRMS/MT with its 30,000 lb payload maneuver begins just after completion of the second orbit. The change in the moments of inertia during this maneuver is about $+9.8\%$ for I_1, $+10.2\%$ for I_3, and no change for I_2. As shown in Fig. 5, the Honeywell controller, with a high attitude control bandwidth of 0.04 rad/s shows significant dynamical interaction, in particular for the CMG momentum, during the translational maneuver. Since the overall inertia changes are within the robustness bounds of the JSC controller even with nonadaptive gains, the JSC controller is still stable after the maneuver, as shown in Fig. 6. It can also be seen that the JSC controller with a low attitude control bandwidth shows little interaction during the MRMS/MT translation.

Case III: Seven-Bay Translation Along the Pitch Axis

In case III, the MRMS/MT/payload moves seven bays. The maneuver starts at the completion of the second orbit. The change in the moments of inertia during this maneuver is about $+33.3\%$ for I_1, $+28.8\%$ for I_3, and no change for I_2. As shown in Fig. 7, the JSC controller without gain adjustment becomes unstable in this case because of the significant inertia changes beyond its robustness bounds. However, the Honeywell controller with adaptive gains shows excellent performance as the inertia changes. The dynamical interaction during the maneuver is still a problem for the Honeywell

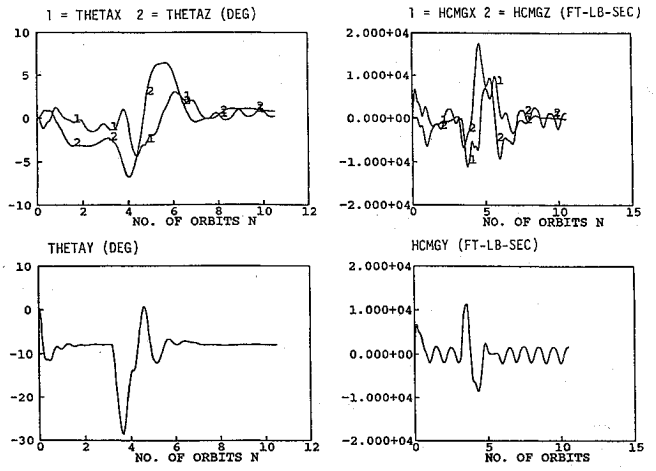

Fig. 8 Case IV with the JSC controller.

controller because of its high bandwidth attitude control loop. The time responses of the Honeywell controller for this case are very similar to those in Fig. 5, hence, they are not included here.

Case IV: 180-deg Slew Maneuver About the Pitch Axis

Case IV consists of a 180-deg slewing of the payload about the y axis. Translation of the MRMS/MT does not occur in this case. The mass center offset of the payload during the slew maneuver is approximately 50 ft. The maximum change for the moments of inertia during this slew maneuver is about +2.97% for I_1, +37.5% for I_2, and 7.6% for I_3. During the slew maneuver, the maximum excursion of the pitch attitude of both controllers is about −28 deg, as can be seen in Fig. 8 for the JSC controller. After the maneuver, pitch attitude returns back to −18 deg TEA. Large transient responses are observed in the attitude changes in all three axes due to the payload slew maneuver.

Summary

Based on the results of a multibody simulation study, the following are the general comments for both controllers. As shown in Fig. 5 for case II, the Honeywell controller with a high attitude control bandwidth shows significant dynamical interactions during the MRMS/MT translational maneuver. The attitude control bandwidth of 0.04 rad/s selected in Ref. 1 is probably too high for the MRMS/MT operations. A preliminary redesign indicates that lowering the attitude control bandwidth improves the internal disturbance attenuation characteristics. However, the attitude control bandwidth of the classical controller[1] cannot be lowered too much since the control system is designed for large spectral separation between the inner attitude control loop and the outer momentum control loop. Also, this classical multiloop design approach makes the incorporation of disturbance rejection filtering more difficult. However, the adaptive nature of the Honeywell controller based on an analytical pole-placement approach shows excellent performance regardless of inertia changes.

The JSC controller shows an excellent response to the internal disturbance caused by the MRMS/MT translational maneuver, because of its relatively low attitude control bandwidth. The modern LQR design method is considered necessary for the integrated design of both attitude control and momentum control loops. The LQR technique also makes the disturbance filter design rather trivial. However, an LQR-based controller, in general, may need proper gain scheduling or real-time LQR gain computation if autonomous capability similar to that of the Honeywell controller is desired. Further investigation into developing a combined modern and classical design approach to integrated attitude control and CMG momentum management is needed.

Conclusions

The effects of the motion of the mobile remote manipulator system and mobile transporter and its payload on the attitude control and momentum management of the Space Station Freedom have been investigated. It was shown that a classical controller designed using the spectral separation concept is sensitive to the payload maneuver because of its relatively high attitude control bandwidth. It was also shown that the most significant impact due to the motion of a large payload is the resultant change in the overall inertia property, whereas a controller with high attitude control bandwidth shows significant transient effects during the payload maneuvers. The study results indicate that some form of adaptive/robust control is necessary to account for the large changes in the inertia property due to the motion of the mobile transporter and its large payload.

Acknowledgments

The authors gratefully acknowledge the technical assistance of Buddy Schubele at Dynacs Engineering Co., John Yeichner at Honeywell Inc., Florida, and John Sunkel at NASA Johnson Space Center. The first author would like to express special thanks to Arthur E. Bryson Jr., at Stanford University, who taught him the importance of practical control design, and who emphasized *both* classical and modern state-space control approaches.

References

[1]Yeichner, J.A., Lee, J.F., and Barrows, D., "Overview of Space Station Attitude Control System with Active Momentum Management," AAS Paper 88-044, 11th Annual AAS Guidance and Control Conference, 1988.

[2]Woo, H.H., Morgan, H.D., and Falangas, E.T., "Momentum Management and Attitude Control Design for a Space Station," *Journal of Guidance, Control, and Dynamics*, Vol. 11, No. 1, 1988, pp. 19–25.

[3]Wie, B., Byun, K.W., Warren, W., Geller, D., Long, D., and Sunkel, J., "New Approach to Attitude/Momentum Control of the Space Station," *Journal of Guidance, Control, and Dynamics*, Vol. 12, No. 5, 1989, pp. 714–722.

[4]Warren, V.W., Wie, B., and Geller, D., "Periodic-Disturbance Accommodating Control of the Space Station for Asymptotic Momentum Management," AIAA Paper 89-3476; also, *Journal of Guidance, Control, and Dynamics*, Vol. 13, No. 6, pp. 984–992.

[5]Harduvell, J.T., "Comparison of Continuous Momentum Control Approaches for the Space Station," McDonnell Douglas, Space Station Div., Internal Memo, A95-J845-JTH-M-8802099, Sept. 1988.

[6]Yeichner, J.A., and Strickland, J., "Space Station CMG Momentum Management System," Space Station GN&C Technical Exchange Meeting, NASA Johnson Space Center, Houston, TX, March 1989.

[7]Roithmayr, C., "Momentum Manager Performance with Mobile Transporter," Space Station GN&C Technical Exchange Meeting, NASA Johnson Space Center, Houston, TX, March 1989.

[8]Sunkel, J.W., and Shieh, L.S., "An Optimal Momentum Management Controller for the Space Station," AIAA Paper 89-3474; also, *Journal of Guidance, Control, and Dynamics* (to be published).

[9]"Impact of Mobile Remote Manipulator System Operations on Attitude Control and Momentum Management System for the Phase I Space Station," NASA Langley Research Center and Dynacs Engineering Co., Inc., Tech. Rept. Dec. 1988.

[10]Singh, R., Schubele, B., and Sunkel, J., "Computationally Efficient Algorithm for the Dynamics of Multi-Link Mechanism," AIAA Paper 89-3527, Aug. 1989.

[11]Bryson, A. E., Jr., *Control of Spacecraft and Aircraft*, class notes, Dept. of Aeronautics and Astronautics, Stanford Univ., Stanford, CA, April 1987 (to be published as a textbook).